

Increasing the Bearing Capacity of Shallow Foundations on Soft Soil After the Installation of Micro-Piles

Isnaniati^{1,2,*}, Indrasurya B. Mochtar²

¹Faculty of Engineering, University of Muhammadiyah, Surabaya, INDONESIA

²Faculty of Civil Engineering, Environmental and Geo Engineering, Institut Teknologi Sepuluh Nopember, Surabaya, INDONESIA

*Corresponding author: isnaniati@ft.um-surabaya.ac.id

SUBMITTED 24 October 2022 REVISED 15 March 2023 ACCEPTED 20 April 2023

ABSTRACT The bearing capacity of shallow foundations on soft soils can generally be estimated based on Local Shear Failure (Terzaghi theory). Several researchers previously stated that the installation of micro-piles on the failure area (slide) can increase the shear strength of the soil. This can be followed up by providing micro-pile reinforcement to prevent lateral soil movement. Therefore, this research was conducted to increase the bearing capacity of shallow foundations on medium-consistency soft clay soils that have been reinforced with micro piles. The research was conducted using modeling in the laboratory with a scale of 1:30. The soil sample used was kaolin clay made from slurry made from kaolin powder with a water content ($w_c = 1.77$ LL), liquid limit (LL = 62.35%) and sample diameter ($d = 33$ cm). The slurry was formed by compacting at a medium consistency level with an undrained cohesion value ($c_u = 0.397$ kg cm⁻²). The micro-pile material in the form of apus bamboo was installed, varying in diameter (d) 0.2 cm (0.027 B), 0.3 cm (0.04 B), and 0.5 cm (0.07 B); sum (n) 4, 9, 16, and 25; and length (L) 10 cm (1.33B), 13 cm (1.73B), and 16 cm (2.13B) micro-piles. While the foundation model uses a square foundation $B \times B$ with $B = 7.5$ cm. The tests were carried out before and after the micro-piles were reinforced with a soil shear failure test. The results showed that a decrease of 0.1B caused an increase in the ultimate bearing capacity of the micro-pile ($q_{ult-empirical, 0.1B}$) from the ultimate bearing capacity before installing the micro-pile. This value is then used to determine the ultimate bearing capacity ratio so that $R_{q,0.1B} = q_{ult-empirical,0.1B}/q_{ult-Terzaghi}$ with the optimum bearing capacity ratio occurring at $R_{q,0.1B}$ with $n_3 = 16$, $d_2 = 0.04B$, $L_2 = 1.73B$.

KEYWORDS Bearing Capacity Of Shallow Foundations; Reinforcement Of Micro-Piles; Soft Soils; Laboratory Models; Slurry

© The Author(s) 2023. This article is distributed under a Creative Commons Attribution-ShareAlike 4.0 International license.

1 INTRODUCTION

Soft soils are generally characterized by several factors that contribute to their poor bearing capacity and substantial settlements. This can be attributed to their high-water content, void ratio, and minimal resistance between the soil particles, all of which result in a weak soil strength. The soil lacks the necessary strength to withstand the applied loads, leading to a low carrying capacity. Furthermore, loading the soil causes a reduction in the void ratio and land subsidence. Therefore, the greater the load applied, the greater the settlement.

Figure 1a shows the application of load (q) on shallow foundations with an expected gradual increase in the foundation settlement as the load increases. The soils on both sides of the foundation bulged, and the slip surface extended to the ground surface when the load q reached the q -ultimate ($q =$

q_{ult}), as indicated in Figure 1a. This failure surface is referred to as general shear failure (Terzaghi et al., 1996) and is typically observed in foundations constructed on granular and stiffer soils. The construction of a shallow foundation on relatively soft soils can lead to local shear failure, causing the triangle wedge underneath the foundation to move downward, and the failed surface ending somewhere within the soil as, presented in Figure 1b. The curves of the load-settlement relationship for general and local shear failures are represented by Curve-I and Curve II, respectively, in Figure 1c (Terzaghi et al., 1996).

The pattern of local shear failure, presented as curve II in Figure 1c, exhibited the same trend as the results obtained when testing on medium clay soils before the installation of micro-piles. This served as the basis for the analysis in this study to

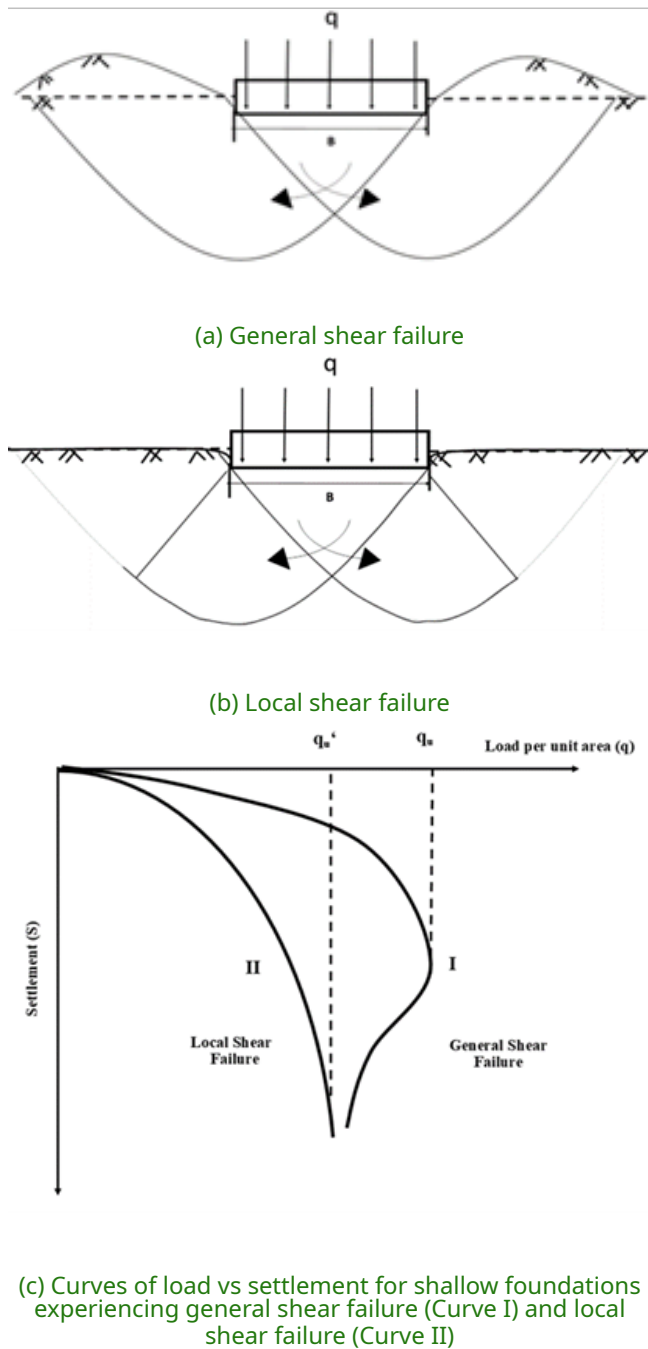


Figure 1 Illustration of bearing capacity failure of the soil underneath (Terzaghi et al., 1996; Das, 2010)

determine the testing results of soft clay samples. The cohesion value for local shear failure was 2/3 of the undrained cohesion ($c = 2/3c_u$) (Terzaghi et al., 1996; Das, 2010), as depicted in the Terzaghi failure model shown in Figure 1b. The general formula for the ultimate support of shallow foundation with a square shape is as follows:

$$q_{ult} = 1.3cN_c + \gamma DfN_q + 0.3B\gamma N_\gamma \quad (1)$$

The bearing capacity of shallow foundations can be improved through the implementation of

micro-piles reinforcement to prevent lateral soil movement. Numerical studies conducted on clay and sandy soils using micro-piles reinforcement under shallow foundations showed an increase in soil carrying capacity compared to soil without micro-piles (Alnuaim et al., 2016).

Another numerical study investigated the use of micro-piles with the deep soil mixing (DSM) method to mitigate the decrease in the bearing capacity of shallow foundations caused by liquefaction, employing FLAC3D. The results indicated that the increase in seismic carrying capacity was greater with longer DSM, however, the larger the diameter of the DSM, the smaller the bearing capacity of the shallow foundations (Hasheminezhad and Bahadori, 2022).

In addition to numerical study, laboratory experiments have also been conducted on models of shallow foundations in clay soils, incorporating different diameters and lengths of micro-piles. The results showed an increase in the carrying capacity of soft clay soils by up to 2.2 times compared to those without micropile reinforcement (Suroso, 2008, 2010).

Efforts were made to strengthen previous studies by installing micro-piles under a shallow foundation at different slope angles (Θ) of 0° , 15° , 30° , 45° , and 60° . The largest increase in the bearing capacity of the soils was observed in micro-piles placed vertically ($\Theta = 0^\circ$), while those with a greater angle of inclination had smaller values (Tsukada et al., 2006).

Several other studies involving laboratory and numerical models have also been conducted in addition to those previously mentioned. This particular study utilized laboratory model testing and GeoStudio 2D element analysis to examine fly ash reinforcement on shallow foundations using micro-piles with varying length-to-diameter ratios ($L/D = 60; 80; 100; 120$). The results showed that each case of the bearing capacity ratio (BCR) exceeded 1 (Shah et al., 2021).

Field studies have also been conducted with post-grouting micro-piles on soft soil, a case study of transmission leaning tower foundations in China. The results showed an increase in axial compressive bearing capacity of 2.5 times non-grouting micro-piles (Wen et al., 2020).

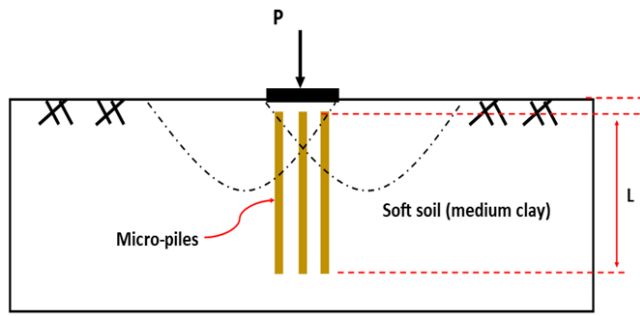


Figure 2 Illustration of micro-piles installation to resist lateral forces

The data provided highlighted the necessity for further studies on the use of micro-piles as reinforcement to resist lateral movement, as shown in Figure 2. Micropiles are used as reinforcement to increase the ultimate bearing capacity of shallow foundations through variations installed in length (L), diameter (d) and number (n). This study focused on soft soils, specifically medium clay consistency. The relationship between the length, diameter and number of devices to the ratio of ultimate bearing capacity at 0.1 B settlement ($R_{q0.1B} = Q_{ult-empiris,0.1B} / Q_{ult-local\ shear\ Terzaghi}$) was discussed, where B was the width of the foundation. The study addressed the following aspects:

1. The effect of the number of micro-piles on increasing the ultimate bearing capacity of shallow foundations.
2. The effect of micro-piles length on increasing the ultimate bearing capacity of shallow foundations.
3. The effect of micro-piles diameter on increasing the ultimate bearing capacity of shallow foundations.

To ensure even settlement, it is crucial to evenly distribute the installed micro-piles with a square number of micro-piles ($n_1 = 2^2 = 4$; $n_2 = 3^2 = 9$; $n_3 = 3^2 = 9$; $n_3 = 4^2 = 16$; $n_4 = 5^2 = 25$). The top end of the micro-piles should not be connected to the shallow foundation to allow the micro-piles resist lateral movement, in accordance with the objectives of this study. The novelty of this study lied in the fact that micro-piles as reinforcement intersected the failure plane, withstood lateral movements, increased the shear strength of the soil, thereby enhancing the ultimate bearing capacity of shallow foundations.

2 METHODS

This study used a scale of 1:30 as a comparison between test objects in the laboratory and reality in the field. The determination of the scale was based on the experimental scale by considering the laboratory capacity, test tubes and sample material, as well as supporting literature based on previous research (Alfani et al., 2022). In building scaling, there were no definite criteria regarding the scale range used, but most laboratory experiments have been successful with a scale range of 1:10 to 1:50 depending on the tested parameters and laboratory capacity (Esmailpour et al., 2023). Also, micro-piles testing as a reinforcement for shallow foundations on soft soils to increase ultimate bearing capacity used a scale value of 1:30 where 1 cm in the laboratory represents 30 cm in field or actual conditions, as shown in Table 1.

The materials included medium consistency clay and micro-piles used with apus bamboo *Gigantochloa apus* from East Java, Indonesia. Apus bamboo was used because it belongs to a strong class II, hence it can be classified as a construction class material (Manik et al., 2017). The bamboo also has the best type of structural gradation due to its maximum compressive load carrying capacity (F_c) which can be precisely and accurately predicted (Bahtiar et al., 2019). Apus bamboo is good for use on trees of at least 2 years old (Ye and Fu, 2018). The laboratory test results based on SNI 03-359-1995 and ASTM D-143 showed average values of 0.2 cm and 0.3 cm for micropiles diameters, 0.5 cm for bending stresses (σ_{lt}) of 3900 kg cm^{-2} , elastic modulus (E) of $1.89 \times 10^5\text{ kg cm}^{-2}$, torsion moment (MP) of 2.374 kgcm, and strain (ϵ) of 2.574%. The stages involved in this study are as follows:

1. Soil sampling
2. Installation of micro-piles on samples
3. Tests

This study was conducted in a laboratory with the micro-piles varied at different diameters (d) at 0.027B, 0.04B, and 0.07B, numbers (n) at 4, 9, 16, and 25, as well as length (L) at 1.33B, 1.73B, and 2.13B. Furthermore, the micro-piles were placed under a shallow foundation designed in the form of a $B \times B$ square where $B = 7.5\text{ cm}$. The experiment was used to produce the ultimate bearing capacity ratio ($R_{q0.1B} = Q_{ult-empirical0.1B} / Q_{ult-Terzaghi}$),

Table 1. Using a mini-scale laboratory model of 1:30 from the size in the field

Information	notation	Satuan	Laboratory model scale 1/30	Real size in the field
Foundation width	B	cm	7.5	225
The thickness of the iron plate foundation	tp	cm	0.3	9
Foundation depth (t depth)	Df	cm	0	0
Maximum vertical collapse length (Brown, 1994)	D=B	cm	7.5	225
The failure length horizontal direction (left and right side) was measured from the edge of the foundation (Brown, 1994)	Ls	cm	7.5	225
Micro-pile diameter (d1, d2, d3)	d	cm	0,2; 0,3; 0,5 0.027B; 0.04B; 0.07B	6, 9, 15
Micro-pile length (L1, L2, L3)	L	cm	10; 13; 16 1.33B; 1.73B; 2.13B	300; 390; 480
Soil sample height: 0.5+ L3 +2.0 Where, 2.0 cm = vertical settlement space	H1	cm	18.5	555
Soil sample diameter: 2Ls+ B + 10.5 Where, 10.5 cm = anticipating more free left and right side lateral movements	ds	cm	33	675

where, $q_{ult-empirical}$ was obtained from testing the soil samples with and without micro-piles.

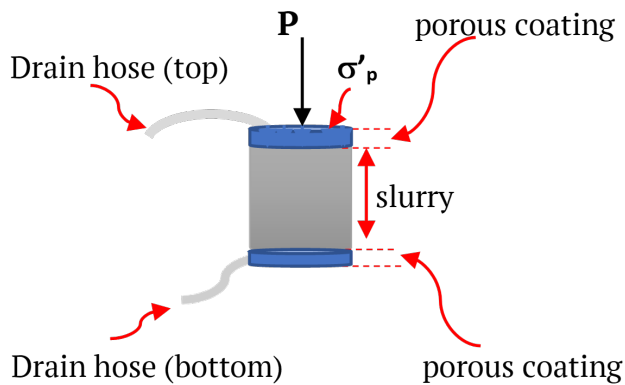
2.1 Soil Sample Production

Clay samples with medium consistency were prepared from kaolin-based slurry using the compression method. The kaolin soil was sourced from the island of Bangka, Indonesia, with a liquid limit (LL) value of 62.35% and a plastic limit (PL) value of 38.33%. The slurry was produced with a water content (w_c) of $1.7 \times LL$ (Lambe and Whitman, 1969) and placed into a tube with a diameter (d) of 33 cm. The production of a sample with $c_u = 0.397 \text{ kg cm}^{-2}$ and water content ($w_c = 53.95\%$) required a load (σ_p') of 1.989 kg cm^{-2} for time (t) of 5 to 7 days. These load and time values were determined from the results of previous experiments. The method for loading the slurry into the tube is illustrated in Figures 3a and b.

Slurry Compression Method Soil samples with a clay medium consistency level were obtained from slurry samples using compression method. An estimate of the c_u value (Ardana, 1999) was initially carried out to determine the magnitude of the vertical effective stress (σ_p'). The magnitude of $\sigma_p' = 1.989 \text{ kg cm}^{-2}$ based on the estimated c_u value was used for the loading test on the sample diameter (d= 7.15 cm; 17 cm). The time needed to compress

the sample was reviewed at the degree of consolidation ($95\% < U < 100\%$). This was to ensure the pore water pressure (u) in the sample returned to hydrostatic pressure ($u = u_o$). The consolidation time took 3 days for thick slurry samples ($H_o = 23 \text{ cm}$) with $d = 7.15 \text{ cm}$, and 2 days for slurry samples of ($H_o = 13 \text{ cm}$) with $d = 17 \text{ cm}$. The compressed diameter sample ($d = 7.15 \text{ cm}$; 17 cm) was subsequently tested for soil shear strength using the Unconfined Compression Test (UCT) and the Vane Shear Test (VST) to determine the true undrained cohesion (c_u).

The test was conducted on four soil samples with a medium clay consistency level. This was carried out to obtain the average c_u values for the two sample diameters (7.15 cm and 17 cm) of 0.395 kg cm^{-2} for UCT and 0.403 kg cm^{-2} for VST. Since the c_u values from the test fell within the range of medium clay consistency level (Umum and Rakyat, 2019), the value of $\sigma_p' = 1,989 \text{ kg cm}^{-2}$ was used as a reference for preparing samples $d = 33 \text{ cm}$. It was subjected to a loading time at the degree of consolidation ($95\% < U < 100\%$), taking a minimum of 5 days for a slurry sample thickness of approximately $H_o = 29 \text{ cm}$. Micro-piles were later installed in the soil samples produced at this stage.



(a) Drainage layer in the slurry sample tube



(b) Compression of the slurry sample

Figure 3 Formation of medium clay samples, $d = 33$ cm

2.2 Micro-pile Installation

The micro-piles were installed under a shallow foundation using the pattern presented in Figure 4, from the outside to the inside direction:

The number of micro-piles installed spread evenly with $n = 2^2 = 4$; $3^2 = 9$; $4^2 = 16$; $5^2 = 25$, ensuring even distribution (no differential settlement) when there was a decrease. The micro-piles were installed starting from the edge point and ending at the inner point to reduce the buildup of excess pore water pressure (due to installation of the

micro-piles) outside the group of micro-piles. This process is illustrated in Figure 5.

The ends of the micro-piles were sharpened before installation to minimize the damage to the soil grain structure. They were plugged vertically, at an angle (θ) of 0° , from the outer side to the inner side. This was aimed at reducing the excess pore water pressure toward the outer area of the micro-piles group caused by the installation process.

The tops of the micro-piles were not directly installed under the foundation plate but kept at a distance of 0.5 cm from the soil surface. This ensured they did not bear any vertical load from the foundation plate, as shown in Figure 6a. The distance between the edge of the foundation plate and the outer cylinder wall of the soil sample was approximately $2B$, as shown in Figure 6b.

The test specimens were left in a closed and moist place for several days (waiting period) after the installation of the micro-piles. This was carried out to restore the initial strength of the soil which was probably disturbed by the installation process and the possible elevation of uneven pore water pressure around the group. The waiting period for each number of micro-piles “ n ” varied. For instance, $n_1 = 4$ required 1 to 2 days, $n_2 = 9$, 2 to 3 days, $n_3 = 16$, 3 to 4 days, and $n_4 = 25$, 5 to 6 days.

Perforated iron was attached to the foundation plate to ensure the load P remained in the midpoint position. The magnitude of P was calculated by multiplying the effective vertical stress by the circular cross-sectional area of the sample ($P = \sigma'_p \cdot \frac{1}{4} \pi d_s^2$).

The next stage after the installation of micro-piles is the Shear Collapse Test.

2.3 Test

This soil shear failure test phase was used to determine the working load at the time of settlement $0.1 \times B$ ($P_{0.1B}$), where B , the width of the foundation, was 7.5 cm (Badan Standarisasi Nasional, 2017). Observations were made with a vertical loading speed set at 15 mm/minute, and the starting position of the loading was confirmed to be at force (P) = 0 Newton. The test was stopped upon experiencing significant deformation or fail-

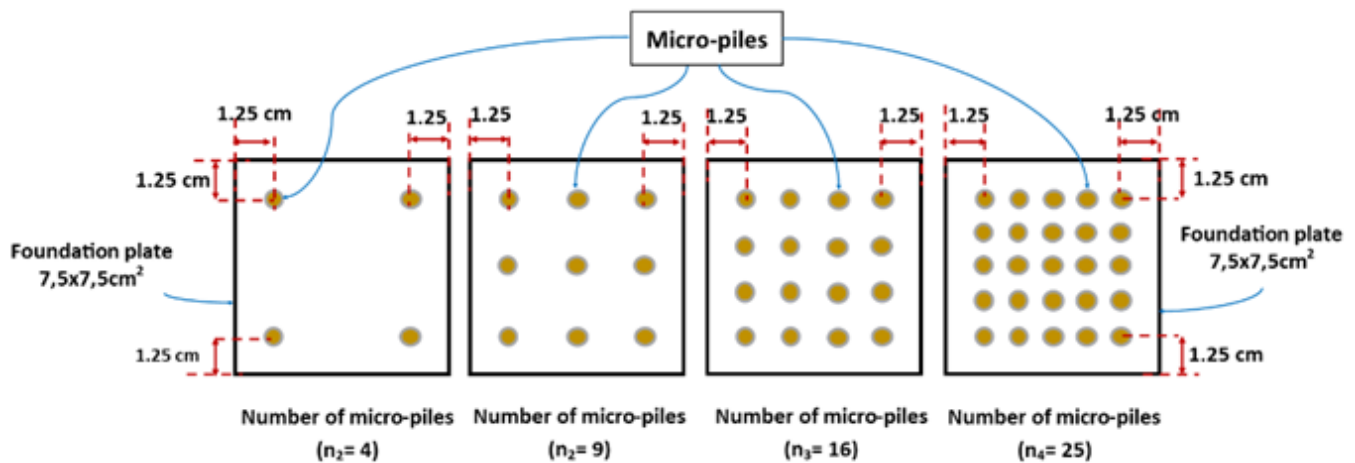


Figure 4 The installation pattern of the micro-piles under a shallow foundation at different numbers (n) = 4, 9, 16, and 25 as well as a distance of 1.2cm from the edge of the foundation to the axle micro-piles

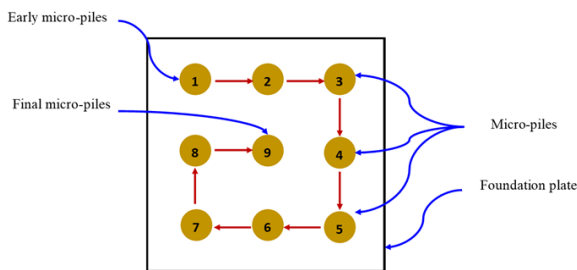


Figure 5 Micro-piles installation order for n= 9

Table 2. Composition of 20 (twenty) samples installed with micro-piles with variations of n, L, d

Length of micro-piles, L (cm)	Number of sample				diameter of micro-piles, d (cm)
	Number of micro-piles, n				
	n1= 4	n2= 9	n3= 16	n4= 25	
L1 = 10 (1.33B)	1	1	1	1	d1 = 0.2 (0.027B)
L2 = 13 (1.73B)	1	1	1	1	d1 = 0.2 (0.027B)
L3 = 16 (2.13B)	1	1	1	1	d1 = 0.2 (0.027B)
L3 = 16 (2.13B)	1	1	1	1	d2 = 0.3 (0.04B)
L3 = 16 (2.13B)	1	1	1	1	d3 = 0.5 (0.07B)

ure, and the load conditions were recorded at a decrease of 0.1 B ($P_{0.1B}$). The test was conducted on twenty samples with micro-piles at different L, d, and n as well as one sample without the reinforcement, as shown in Table 2. The shear failure of micro-piles under shallow foundations on soft soils was tested based on ASTM: C 293-02, as shown in Figure 7.

2.4 Data Analysis

The data from the one sample without micro-piles and the twenty samples with micro-piles installed at different L, d, and n were analyzed to determine the ultimate bearing capacity ratio (R_q), as shown in Table 2. R_q is the ratio of the empirical bearing capacity ($q_{ult-empirical}$) with a 0.1 B reduction to the Terzaghi bearing capacity ($q_{ult-Terzaghi}$). The empirical bearing capacity ($q_{ult-empirical}$) was obtained through the shear failure test conducted on both the sample without micro-piles ($q_{ult-empirical, n=0}$) and those with micro-piles ($q_{ult-empirical, n \neq 0}$). The bearing capacity of Terzaghi ($q_{ult-Terzaghi}$) was determined using the formula for a square foot foundation (Isnaniati, 2017), as presented in Equation 1. The undrained clay soil $\phi = 0^\circ$ produced $N_c = 5.7$, $N_\gamma = 0$, and $N_q = 1$ at $D_f = 0$ m

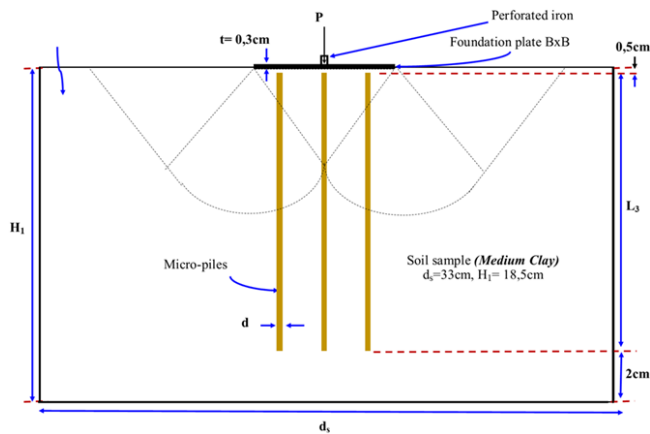
$$q_{ult} = 1,3.c.N_c \tag{2}$$

The c for local shear failure conditions was $2/3c_u$, indicating an ultimate bearing capacity (Terzaghi et al., 1996) of

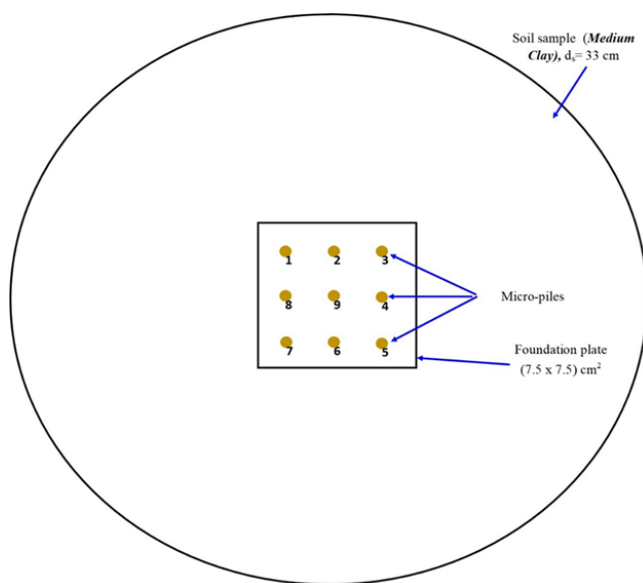
$$q_{ult} = 7,41.c_u \tag{3}$$

3 RESULT AND DISCUSSION

The ratio of the ultimate empirical bearing capacity obtained through 0.1 B reduction (National, 2017) to the ultimate carrying capacity of Terzaghi was determined using $R_{q0.1B} = q_{ult-empirical0.1B}/q_{ult-Terzaghi}$. Figures 8, 9, and 10 show the results based on the variations in the number (n), diameter, ($d_1 = 0.2$ cm), and length (L_1 ,



(a) Sample pieces attached to micro-piles with $n_1 = 9$ and $L_3 = 16 \text{ cm} (= 2.13B)$



(b) Top view of the sample attached to micro-piles with $n_1 = 9$

Figure 6 Micro-piles installed for soil shear collapse test



Figure 7 Shear failure test on medium clay soil samples

L_2, L_3), along with their relationship with the ultimate bearing capacity. This is explained as follows:

1. The empirical bearing capacity at $0.1 B$ subsidence for soil without micro-piles showed only slightly differences from the carrying capacity obtained from the Terzaghi formula, with an average R_q of 0.953. This indicated there was practically a match between Terzaghi's theory (Terzaghi et al., 1996) and the present study.
2. A significant increase was observed for R_q with a greater number of micro-piles, but this increase became insignificant when $n > 16$, resulting in a constant or decreasing R_q value. This indicated both the soil and the number of micro-piles determined the bearing capacity of the foundation, but the R_q stopped increasing at a higher number or high strength of micro-piles. Similar observation were reported in several previous studies (DM-7, N., 1971; Mochtar, n.d.; Rusdiansyah and Mochtar, 2015, 2016)
3. The length (L) of the micro-piles had a relatively small effect on the increase in R_q as shown in Figure 8. The increment in R_q remained small for different lengths (L) but the same number of micro-piles (n). This was probably due to the fact that the 10, 13, and 16 cm lengths practically intersected the shear failure line of the soil under the foundation slab. The effect of micro-piles length on R_q was also presented in Figure 9, where the change in R_q was relatively small for the specified variations of micro-piles length, as further confirmed by Brown (Brown, 1994). The highest R_q was obtained at $L = 13 \text{ cm} (1.73B)$.
4. The effect of micro-piles diameter on the bearing capacity of soil is presented in Figure 10. According (Rusdiansyah and Mochtar, 2016), a relatively small increase in the diameter of micro-piles enhanced the soil's resistance to shear, but this improvement usually became insignificant when a certain diameter was reached. This indicated both the soil and micro-piles contributed to the increase of R_q , but when the micro-piles became too strong due to a relatively large diameter, the shear failure was predominantly determined by the strength of the soil. This consequently led to stagnancy and possible decrease in the R_q value. Figure 10 shows an increase in the R_q

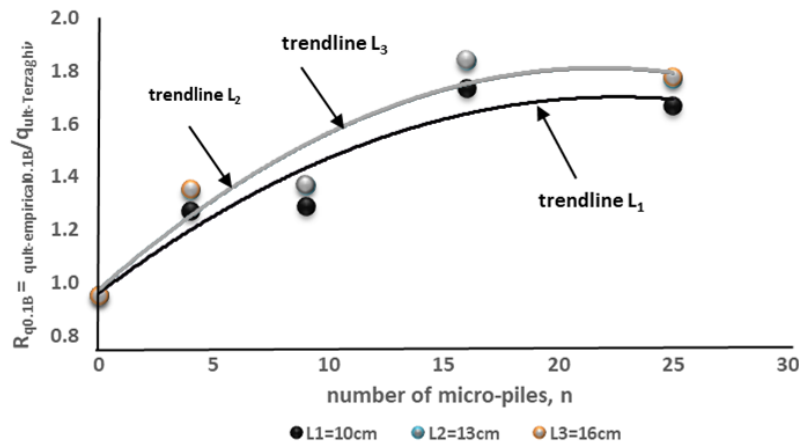


Figure 8 Graph of the relationship between the number of micro-piles "n" to the q_{ult} ratio at a decrease of 0.1B " $R_{q0.1B}$ " with variation L for $d_1 = 0.027B$

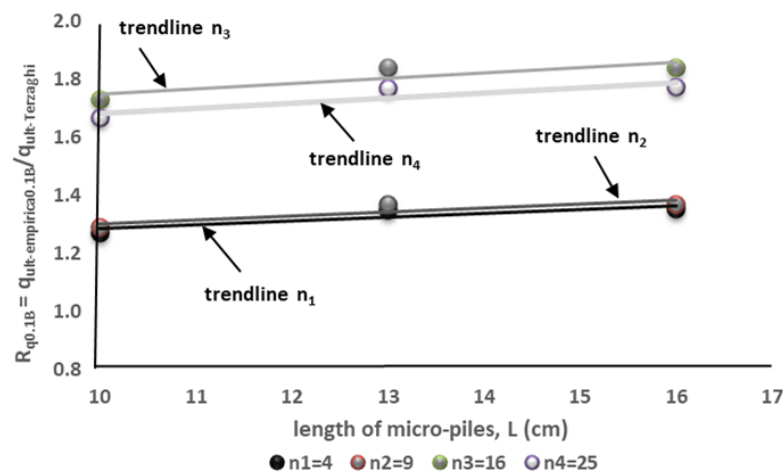


Figure 9 Graph of the relationship between the length of micro-piles "L" to the q_{ult} ratio at 0.1B " $R_{q0.1B}$ " with variation n for $d_1 = 0.027B$

value for $n = 4$ and $n = 9$ when the diameter increases from $d = 0.20$ cm ($= 0.027 B$) to $d = 0.3$ cm ($0.04 B$), followed by a reduction when $d = 0.5$ cm ($0.07 B$). Although the pattern for $n = 16$ and $n = 25$ was not clear, the change in R_q due to the diameter of the micro-piles was relatively less significant compared to the change caused by their number. Moreover, the change in R_q was only significant at a specific diameter d , falling between 0.2 and 0.3 cm.

The results above showed that micro-piles under specific conditions, such as number and length of the piles, had the ability to increase the bearing capacity of the foundation. Similar results have also been reported in several previous studies. Cao et al. (2004) verified the effectiveness of using micro-piles under a shallow foundation, consider-

ing factors such as thickness, pile depth, installation pattern, and number of piles. The study showed that micropile beneath a raft foundation could reduce settlement and bending moment of rafts. In addition, Park et al. (2020) obtained similar results by conducting a centrifuge test. It was found that disconnected rift piles had the same system as the micro-piles in the present study, thereby reducing soil settlement while also affecting its bearing capacity.

Eslami et al. (2012) examined the ratio of the width of the area where disconnected raft piles were installed (using the same system as this study) and the width of the foundation to settlement. The results showed that disconnected raft piles installed under the raft effectively reduced settlement when placed at the center of the foundation.

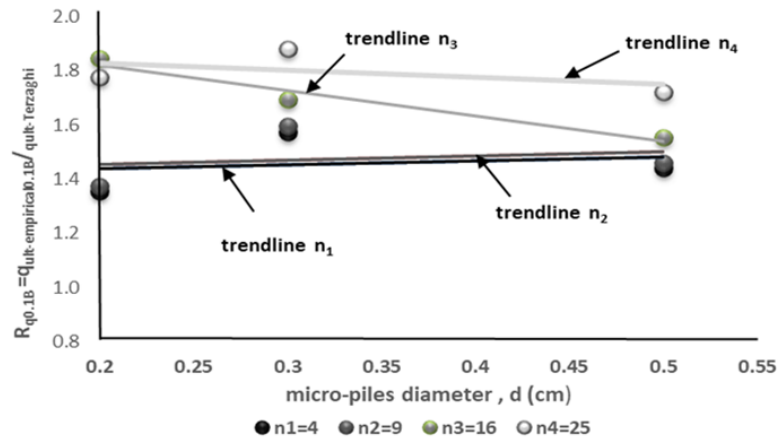


Figure 10 Graph of the relationship between the diameter of micro-piles "d" to the q_{ult} ratio at 0.1B " $R_{q_{0.1B}}$ " with variation n for $L_3 = 2.13B$

The function of pile configuration in raft geometry, as demonstrated in this study, could reduce settlement, particularly when concentrated at the middle of 15-25% of the raft plan area.

These results were consistent with El Sawwaf (2010) which examined sand soil and Reul and Randolph (2004). El Sawwaf explored the ratio of the bearing pressure of a piled raft to that of an unpiled raft at the same settlement level. The results showed that improvements in the bearing pressures at the same settlement level were greater with longer piles. The ratio of the bearing pressure of a piled raft to that of an unpiled raft at the same settlement level initially increased with the increase in pile number. However, the increasing rate and the settlement of rafts became quite small when the number reached a certain value.

In summary, the results showed that micro-piles under raft/shallow foundation could increase the bearing capacity, the increase ratio depending on the number, length, and configuration. These results aligned with previous studies conducted on various soil types using different methods.

4 CONCLUSION

In conclusion, the results obtained from the placement of micro-pile models under a shallow foundation showed that the number "n" of the micro-piles had a significant influence on the increase in the ultimate bearing capacity ratio ($R_{q_{0.1B}}$). The length of the micro-piles had a less significant effect due to the length (L) intersecting the failure

line. A similar pattern was observed for the diameter, where the effect was insignificant after a certain value. Moreover, the highest increase in the average $R_{q_{0.1B}}$ value was observed at $n_3 = 16$, $d_2 = 0.3$ cm (0.04B), and $L_2 = 13$ (1.73B).

DISCLAIMER

The authors declare no conflict of interest.

ACKNOWLEDGMENTS

REFERENCES

- Alfani, A. A., Sugianto, D. N., Indrayanti, E., Ismunarti, D. H. and Widiaratih, R. (2022), 'Model fisik pengaruh armour cylinder concrete pada vertical breakwater terhadap koefisien refleksi gelombang', *Indonesian Journal of Oceanography* 4(1), 23–35.
- Alnuaim, A. M., El Naggat, M. H. and El Naggat, H. (2016), 'Numerical investigation of the performance of micropiled rafts in sand', *Computers and Geotechnics* 77, 91–105.
- Ardana, I. M. D. (1999), 'Effect of effective overburden stress and soil plasticity on the shear strength of undrained very soft consistency clay'.
- Bahtiar, E. T., Imanullah, A. P., Hermawan, D., Nugroho, N. et al. (2019), 'Structural grading of three sympodial bamboo culms (hitam, andong, and tali) subjected to axial compressive load', *Engineering Structures* 181, 233–245.

- Brown (1994), *Engineering and Design Bearing Capacity of Soils*, ASCE, ASCE 1992, Departement of the army-Washington, DC 20314-100.
- Cao, X. D., Wong, I. H. and Chang, M.-F. (2004), 'Behavior of model rafts resting on pile-reinforced sand', *Journal of geotechnical and geoenvironmental engineering* **130**(2), 129–138.
- Das, B. M. (2010), *Principles of Geotechnical Engineering*, 7th edn, 200 First Stamford Place, Suite 400, USA.
- DM-7, N. (1971), *Design Manual, Soil Mechanics, Foundation and Earth*.
- El Sawwaf, M. (2010), 'Experimental study of eccentrically loaded raft with connected and unconnected short piles', *Journal of geotechnical and geoenvironmental engineering* **136**(10), 1394–1402.
- Eslami, A., Veiskarami, M. and Eslami, M. (2012), 'Study on optimized piled-raft foundations (prf) performance with connected and non-connected piles-three case histories', *International Journal of Civil Engineering* **10**(2), 100–111.
- Esmailpour, P., Mamazizi, A. and Madabhusi, G. S. P. (2023), 'An overview of the model container types in physical modeling of geotechnical problems', *Soil Dynamics and Earthquake Engineering* **168**, 107827.
- Hasheminezhad, A. and Bahadori, H. (2022), 'On the deep soil mixing method in the mitigation of liquefaction-induced bearing capacity degradation of shallow foundations', *Geomechanics and Geoengineering* **17**(1), 334–346.
- Isnaniati (2017), 'Contribution of the shape of the pile to the maximum load received by the foundation for foundation planning on clay with surabaya cpt data', *aggregate journal* **2**(1), 21–27.
- Lambe, T. W. and Whitman, R. V. (1969), 'Soil mechanics. john willey & sons', *Inc., New York* **553**.
- Manik, P., Yudo, H. and Siahaan, F. A. (2017), 'Pengaruh susunan dan ukuran bilah bambu petung (*dendrocalamus asper*) dan bambu apus (*gigantochloa apus*) terhadap kekuatan tarik, kekuatan tekan dan kekuatan lentur untuk komponen konstruksi kapal', *Kapal: Jurnal Ilmu Pengetahuan dan Teknologi Kelautan* **14**(3), 94–101.
- Mochtar, N. E. (n.d.), 'Soil improvement'. Available at: https://scholar.google.com/scholar?hl=en&as_sdt=0,5&cluster=2757870835937004426.
- Nasional, B. S. (2017), 'SNI 8460-2017', Per-syaratan perancangan geoteknik.
- Park, H.-J., Ko, K.-W., Song, Y.-H., Song, M.-J., Jin, S., Ha, J.-G. and Kim, D.-S. (2020), 'Centrifuge modeling of disconnected piled raft using vertical pushover tests', *Acta Geotechnica* **15**, 2637–2648.
- Reul, O. and Randolph, M. F. (2004), 'Design strategies for piled rafts subjected to nonuniform vertical loading', *Journal of Geotechnical and Geoenvironmental Engineering* **130**(1), 1–13.
- Rusdiansyah, I. B. M. and Mochtar, N. E. (2015), 'Effect of burrow depth, spacing, and number of micro-piles in increasing the shear resistance of soft soil based on laboratory modeling'.
- Rusdiansyah, I. B. M. and Mochtar, N. E. (2016), 'Study on the increment of shear resistance of soft soil due to vertical piles reinforcement based on modeling in laboratory', *International Journal of Applied Engineering Research* **11**(8), 5934–5942.
- Shah, I. A., Zaid, M., Farooqi, M. A. and Ali, K. (2021), 'Numerical study on micropile stabilized foundation in flyash', *Indian Geotechnical Journal* **51**(5), 1099–1106.
- Suroso, H. M. (2008), 'Alternative for reinforcement soft clay soil using micro-piles with variations in length and diameter of micro-piles', *Jurnal Rekayasa Sipil* **2**(1), 47–61.
- Suroso, M. H. (2010), 'The effect of wooden pile and bamboo slice on the bearing capacity of soft clays', *Journal of Civil Engineering* **4**(3), 161–174.
- Terzaghi, K., Peck, R. B. and Mesri, G. (1996), *Soil mechanics in engineering practice*, John wiley & sons.
- Tsukada, Y., Miura, K., Tsubokawa, Y., Otani, Y. and You, G.-L. (2006), 'Mechanism of bearing capacity of spread footings reinforced with micropiles', *Soils and foundations* **46**(3), 367–376.
- Umum, K. P. and Rakyat, P. (2019), 'Kumpulan korelasi parameter geoteknik dan fondasi', *Ke-menterian Pekerjaan Umum dan Perumahan Rakyat. Jakarta*.

Wen, L., Kong, G., Abuel-Naga, H., Li, Q. and Zhang, Z. (2020), 'Rectification of tilted transmission tower using micropile underpinning method', *Journal of Performance of Constructed Facilities* **34**(1), 04019110.

Ye, F. and Fu, W. P. D. (2018), 'No title', *Journal of Materials in Civil Engineering* **30**. Physical and Mechanical Characterization of Fresh Bamboo for Infrastructure Projects.

[This page is intentionally left blank]